CrossMark

Coupling survey data with drift model results suggests that local spawning is important for *Calanus finmarchicus* production in the Barents Sea

Kristina Øie Kvile [a,*], Øyvind Fiksen [b], Irina Prokopchuk [c], Anders Frugård Opdal [b,d]

[a] *Centre for Ecological and Evolutionary Synthesis (CEES), Department of Biosciences, University of Oslo, PO Box 1066 Blindern, 0316 Oslo, Norway*
[b] *Department of Biology and Hjort Centre for Marine Ecosystem Dynamics, University of Bergen, PO Box 7803, 5020 Bergen, Norway*
[c] *Knipovich Polar Research Institute of Marine Fisheries and Oceanography (PINRO), 6 Academician Knipovich Street, 183038 Murmansk, Russia*
[d] *Uni Research and Hjort Centre for Marine Ecosystem Dynamics, PO Box 7810, 5020 Bergen, Norway*

ABSTRACT

The copepod *Calanus finmarchicus* is an important part of the diet for several large fish stocks feeding in the Atlantic waters of the Barents Sea. Determining the origin of the new generation copepodites present on the Barents Sea shelf in spring can shed light on the importance of local versus imported production of *C. finmarchicus* biomass in this region. In this study, we couple large-scale spatiotemporal survey data (>30 years in both Norwegian Sea and Barents Sea areas) with drift trajectories from a hydrodynamic model to back-calculate and map the spatial distribution of *C. finmarchicus* from copepod to egg, allowing us to identify potential adult spawning areas. Assuming the adult stage emerges from overwintering in the Norwegian Sea, our results suggest that copepodites sampled at the Barents Sea entrance are a mix of locally spawned individuals and long-distance-travellers advected northwards along the Norwegian shelf edge. However, copepodites sampled farther east in the Barents Sea (33°30′E) are most likely spawned on the Barents Sea shelf, potentially from females that have overwintered locally. Our results support that *C. finmarchicus* dynamics in the Barents Sea are not, at least in the short-term, solely driven by advection from the Norwegian Sea, but that local production may be more important than commonly believed.

© 2016 Elsevier B.V. All rights reserved.

1. Introduction

The southwestern Barents Sea is a highly productive area, hosting the world's currently largest stocks of cod (*Gadus morhua*) and capelin (*Mallotus villosus*) (Gjøsæter, 2009). The largest herring stock in world, the Norwegian spring spawning herring (*Clupea harengus*), has its main nursery areas in the Barents Sea (Stenevik et al., 2015). The copepod *Calanus finmarchicus* dominates mesozooplankton biomass in the area (Orlova et al., 2010), and constitutes an important part of the diet of these fish stocks; nauplii and younger copepodite stages for various larval and juvenile fish (e.g. cod, herring) and older copepodite stages and adults for adult pelagic fish (e.g. herring, capelin) (Loeng and Drinkwater, 2007; Melle et al., 2004).

It has been suggested that advection from the Norwegian Sea is the dominant source of *C. finmarchicus* biomass in the Barents Sea (Edvardsen et al., 2003b; Helle, 2000; Skjoldal and Rey, 1989; Torgersen and Huse, 2005). The deep basins of the Norwegian Sea are the main overwintering areas of the species in the Northeast Atlantic,

and spawning takes place in the upper water masses when adults emerge in early spring (Melle et al., 2014). Depending on ambient ocean current dynamics, the new generation might be transported out of the Norwegian Sea gyres and into the Barents Sea (Edvardsen et al., 2003a; Samuelsen et al., 2009; Torgersen and Huse, 2005). The dominant surface currents in the area are the North Atlantic Current (NAC), which brings relatively warm and saline Atlantic water northward with branches into the Barents Sea, and the cooler and fresher Norwegian Coastal Current (NCC), which follows the Norwegian coastline into the Barents Sea (Loeng, 1991; Blindheim, 2004).

Several studies have used oceanographic particle tracking to investigate the degree of retention or export of *C. finmarchicus* in the Norwegian Sea. Bryant et al. (1998) found that *C. finmarchicus* populations could be retained for several years within the Norwegian Sea gyres, but individuals present north of these gyres were rapidly flushed out, potentially into the Barents Sea. Torgersen and Huse (2005) found on the other hand that zooplankton advection into the Barents Sea was almost exclusively from the Norwegian continental shelf, but hypothesised that the coarse resolution of the oceanographic model (20 × 20 km) could cause an underestimation of transport from the Norwegian Sea onto the Norwegian shelf. This was supported by

Samuelsen et al. (2009), who observed an overall increase in cross-shelf transport when applying an embedded model with finer grid resolution (4.5 × 4.5 km).

Contrary to the idea of the Barents Sea as a sink of zooplankton advected from the Norwegian Sea, it has recently been estimated that 67–77% of zooplankton production in the Barents Sea is local (Dalpadado et al., 2012; Skaret et al., 2014). In this study, we couple output from a hydrodynamic model with large-scale biological survey data (>30 years in both Norwegian Sea and Barents Sea areas) to find the origin of *C. finmarchicus* individuals observed in the Barents Sea.

2. Materials and methods

2.1. Overview of the approach

To estimate *C. finmarchicus* spawning areas, we use the following approach: (1) Drift particles representing the new generation of *C. finmarchicus* (G1) forward in time, (2) sample particles present at the time and location of observed *C. finmarchicus* copepodites representing endpoints of modelled drift trajectories, (3) estimate ages of observed copepodites and (4) estimate the spatial distribution of eggs, and thus potential adult spawning locations, from the particles' locations at the observed copepodites' estimated spawning days (Fig. 1). Below we describe in detail the biological data, the particle tracking procedure and the approach used to estimate spawning locations.

2.2. Survey data

Knipovich Polar Research Institute of Marine Fisheries and Oceanography (PINRO, Murmansk, Russia) collected stage-specific abundance data (ind. m^{-3}) of *C. finmarchicus* during bi-annual surveys between 1959 and 1992 (described in Kvile et al., 2014; Nesterova, 1990). Samples were collected with a Juday plankton net (37 cm diameter opening, 180 μm mesh size) with a closing mechanism. Since in the present study we were interested in observations of the new generation (G1), we focused on data of copepodite stages CI–CIV collected in spring (mid-April to late May). This period covers the mid–late peak period of stages CI–CIII and early accumulation of stage CIV for southwestern parts of the study area, and the early peak period of these stages for northeastern

parts of the study area (Kvile et al., 2014). Since our focus was to estimate spawning areas for the new generation spawned in spring, we did not include information on the stages CV–CVI, which likely belong to the parental generation emerging from overwintering (G0). Naupliar stages, which due to their small size are under-sampled by the mesh size used (Hernroth, 1987; Nichols and Thompson, 1991), were also excluded from the analyses.

Further, we only used data collected in the upper water column (0–60 m depth), corresponding to the depth layer with highest abundances of young copepodites during the growth season (Dale and Kaartvedt, 2000; Kvile et al., 2014; Unstad and Tande, 1991). To avoid bias due to inter-annual variation in survey coverage, we only included data from repeatedly sampled transects, and within these transects, we only included survey stations sampled at least as many times as the average for that transect. This gave us three off-shelf transects and four on-shelf transects to work with (Fig. 2), and a minimum number of stations sampled per year ranging from 4 (NS·Open3) to 14 (Kola) per transect. The number of stations sampled varied between years, and the total number of stations per year ranged from a minimum of 6 (1959, only one transect included) to 66 (1975, all transects included).

The survey generally covered the transects in a southwest–northeast direction, starting in the southernmost Norwegian Sea transect in mid–late April, and ending with the easternmost Barents Sea transects in mid–late May (Fig. 2., see also Kvile et al., 2014). On average, both the total copepodite abundance (CI–CIV) and the contribution of the youngest copepodites (CI–CII) to the total abundance were higher at the Barents Sea transects compared to the Norwegian Sea transects (Fig. 2).

2.3. Particle-tracking procedure

To simulate past ocean current dynamics in the Norwegian Sea–Barents Sea area, we extracted flow fields from a numerical ocean model hindcast archive (Lien et al., 2013), coupled to a regional ocean model system (ROMS, Haidvogel et al., 2008) with atmospheric forcing from the NORA10 archive (Reistad et al., 2011). This archive provides hydrographic information for the Nordic Seas at daily intervals from 1959 to 2014, with 4 × 4 km horizontal resolution and 32-layer terrain following vertical resolution, and has been shown to realistically reproduce observed hydrographic conditions and circulation in these areas (Lien et
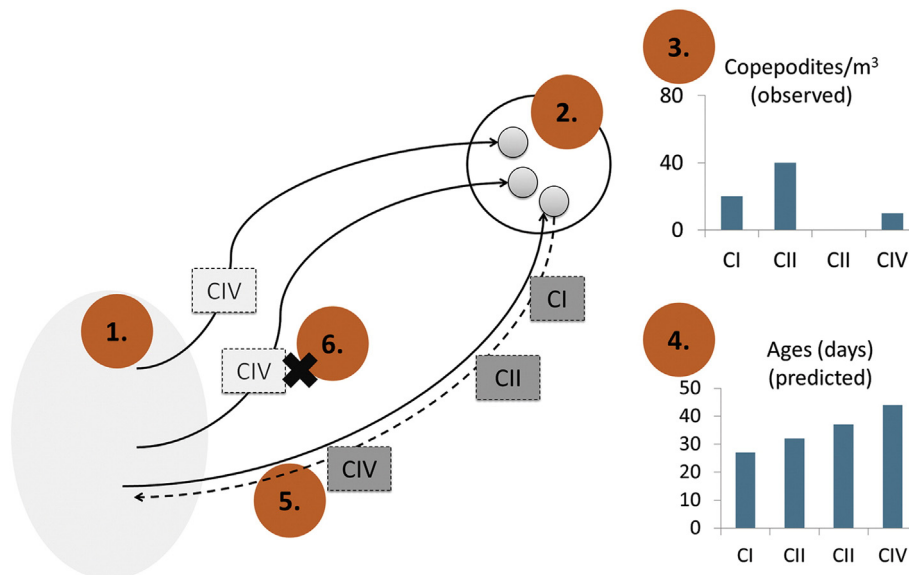
Fig. 1. The approach used to estimate spawning locations. Particles representing the new generation (G1) *C. finmarchicus* are released and advected from the Norwegian Sea in spring (1). Particles are sampled at the time and location of actual survey stations (2). Based on the observed distribution of G1 copepodites at the station (3) and their predicted ages from temperature-dependent development functions (4), we can estimate potential spawning locations as the sampled particles' positions at the estimated stage-specific spawning days (5). We calculate average spawning locations for each stage sampled in a station as the centre of gravity of the stage-specific spawning locations of all particles sampled (shown as a cross for stage CIV), (6).
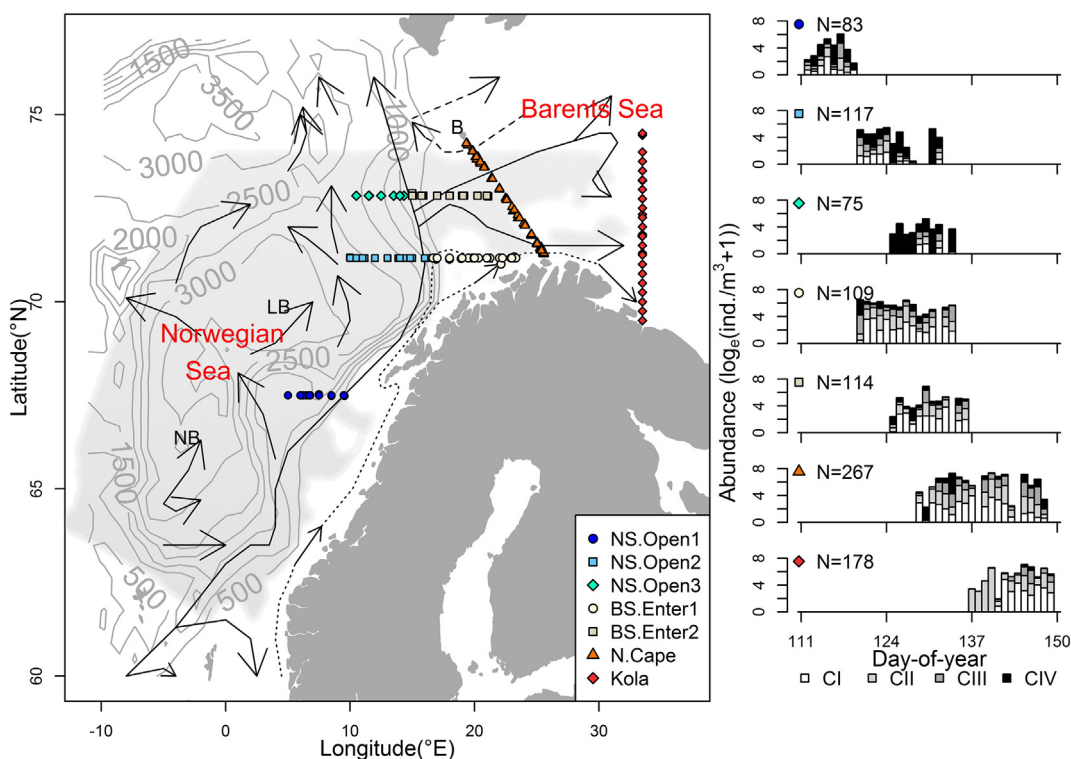
Fig. 2. Survey area (left) and observed copepodite abundances at the survey transects (right). Left: The Norwegian Sea and Barents Sea with depth contours at every 500 m and the main surface currents indicated. Survey transects are marked with different symbols. Solid arrows: North Atlantic Current; dotted arrows: Norwegian Coastal Current; dashed arrows: Arctic water currents; NB: Norwegian Basin; LB: Lofoten Basin; B: Bjørnøya; grey shaded area: particle seeding area. Right: Natural logarithm of the mean pooled abundance of copepodite stages CI–CIV observed per survey day (day-of-year, counting from 1st of January). The survey generally followed a southwest–northeast direction, starting in the Norwegian Sea in mid–late April and ending in the Barents Sea in mid–late May. The contribution of different stages to the total abundance is indicated. N: number of samples with at least one copepodite stage present, pooled for all years.

al., 2013). Particles representing the new generation of *C. finmarchicus* (G1), spawned by females recently ascended from overwintering (G0), were distributed homogenously within the Norwegian Sea (Fig. 2). The distribution was constrained to avoid geographical bias regarding the origin of parents, assuming that shelf areas are too shallow to be important overwintering sites (Hjøllo et al., 2012; Samuelsen et al., 2009). The seeding area was defined as every grid cell in the Norwegian Sea with bottom depth > 500 m, from the north of Shetland and the Faroese Islands to the east of Iceland and Jan. Mayen, south of 74°N (Fig. 2). Each particle was seeded in the centre of a grid cell and fixed at 20 m depth, resulting in a total of 57,869 particles simulated per year.

Particles were released 1st of March every year between 1959 and 1992. This coincides approximately with the start of the phytoplankton spring bloom (pre-bloom) in the Norwegian Sea (Rey, 2004). According to observations in the Norwegian Sea, *C. finmarchicus* egg production is usually initiated during the pre-bloom phase (March–April), and peaks during the main bloom period (May) (Melle et al., 2014, 2004; Niehoff et al., 1999; Stenevik et al., 2007). To test for sensitivity to assumptions in the setup of the particle-tracking model, we also ran the model with deeper and shallower particle depths (20 m ± 10 m), earlier and later release dates (March 1st ± 15 days) and with the seeding area including grid cells with shallower bottom depth (>300 m, Fig. A1 in Appendix A).

To record particle drift trajectories and ambient temperature exposure, we applied a Lagrangian particle-tracking procedure (Ådlandsvik and Sundby, 1994). The particles were advected horizontally according to the velocities at their positions, using a Runge Kutta 4th order scheme with no diffusion. The horizontal resolution of the ocean model may be too coarse to resolve mesoscale eddies in the Barents Sea, where the Rossby radius can be as small as 1–2 km (Lien et al., 2013). Since small-scale variability can influence off shelf–on shelf transport (Samuelsen et al., 2009), we conducted a sensitivity test including random diffusion of the particles to compensate for this potential bias. The

diffusion coefficient was set to 100 m² s⁻¹, which was found to be reasonable for cod larvae drift in the area (Ådlandsvik and Sundby, 1994).

2.4. Back-calculation of spawning locations

After drifting for up to three months, particles were "sampled" at the time and position of survey stations, within a three-day interval and 20 km radius. Thus, for each survey station, in addition to the data of observed copepodites, we obtained information on the number of simulated particles present at the time of the survey and their past trajectories. We back-calculated the approximate age (in days) of observed copepodite stages CI–CIV in each survey station using the Belehrádek temperature function $D = a(T - \alpha)^b$, where D is development time (days), T is temperature (°C), α and b are constants, and a is a stage-specific parameter (Campbell et al., 2001). The function gives the time between the median day of the egg period and the point when 50% of the copepods have reached a specific stage. For every particle sampled in a station, we estimated stage-specific development times using the temperatures experienced by the particle in question, starting with the ambient temperature during the last day of drift and for every preceding day updating the stage duration estimates and the fraction of the total stage durations obtained until all stages back to the egg stage were completed.

We identified potential spawning locations, i.e. locations where the observed copepodite stages could have been present as eggs, by first back-calculating the positions of particles sampled at a given station to the estimated (particle-specific) spawning dates. Since up to four relevant copepodite stages with increasing ages could be present in a station, up to four different locations could be estimated from each particle trajectory, with older stages originating farther upstream than younger stages. We then estimated potential spawning locations (one for each copepodite stage present in a survey station) as the average (centre of gravity) of these stage- and particle-specific locations, giving all

particles sampled in a station equal weight. If no particles reached a station at the time of the survey, no back-calculated egg locations could be derived.

We tested the sensitivity of the results to particle drift depth, release day, release location and implementation of particle diffusion by comparing the following properties per transect:

1. Total number of particles sampled in the stations at the transect
2. Mean drift distance (km) from egg to copepodite stage CIV, i.e. the mean straight-line distance between the survey stations and their respective back-calculated spawning locations for stage CIV
3. Mean development time (days) from egg to copepodite stage CIV
4. Percentage of back-calculated spawning locations situated on the shelf (bottom depth < 500 m)

We also computed the Spearman rank correlations between year-to-year variation in the properties listed above and the winter (December–March) North Atlantic Oscillation (NAO) index (Hurrell and National Center for Atmospheric Research Staff, 2013), which is known to reflect climate variation in the Atlantic waters of the Barents Sea (Ottersen and Stenseth, 2001). In the significance test for the correlation, the effective number of degrees of freedom was adjusted to account for autocorrelation in the time-series following the method described by Quenouille (1952), modified by Pyper and Peterman (1998).

3. Results

3.1. Spawning locations and egg to copepodite transport

The back-calculated spawning locations for *C. finmarchicus* copepodites stages CI–CIV sampled in the different transects are displayed in Fig. 3 (for all years) and Fig. A2 in Appendix A (per year). In the off-shelf Norwegian Sea, the back-calculated spawning locations
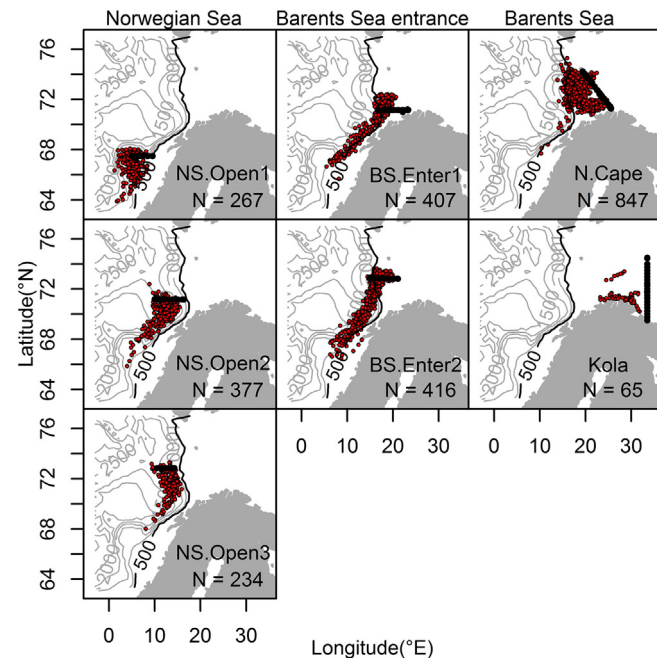
Fig. 3. Back-calculated potential spawning locations (red circles) for different transects (black circles), pooled for all years and copepodite stages (CI–CIV). Each red circle represents the estimated (centre of gravity) spawning location for one copepodite stage observed in one survey station. N: total number of back-calculated spawning locations (the product of the number of survey stations receiving particles and the number of copepodite stages observed in the stations). The 500 m depth contour marks the approximate division between the off-shelf Norwegian Sea and the on-shelf Barents Sea/Norwegian continental shelf. (For interpretation of the references to colour in this figure legend, the reader is referred to the web version of this article.)

in some years formed a relatively circular pattern around the transects, and in other years extended in a long belt along the shelf edge south of the transects and/or south of the Lofoten Basin. For the two transects at the Barents Sea entrance, spawning locations often stretched far south along the shelf edge, and a varying number of origins were situated on the shelf between years [in total 67% and 36% for the southern and northern Barents Sea entrance transects, respectively (Table 1)]. Eggs later appearing as copepodites at the Barents Sea North Cape transect were spawned mainly on the Barents Sea shelf [over 90% of the back-calculated spawning locations were situated on the shelf (Table 1)]. For the Kola transect (33°30′E), all estimated spawning locations were restricted to the Barents Sea shelf. However, this was based on a total of only 30 particles sampled in 18 different stations in 1973 and 1975. For the other years, no particles reached the Kola transect, meaning the observed copepodites could not have originated from eggs spawned in the Norwegian Sea. The estimated total potential spawning locations, i.e. the back-calculated spawning locations from all particles sampled per station in the different transects are shown in Fig. A3 in Appendix A.

To test how far into the Barents Sea it is likely to find copepodites spawned in the Norwegian Sea, we mapped the distribution of particles initially released in the Norwegian Sea which were present in the Barents Sea after 42 days of drift (the average estimated development time of stage CIV at the Kola transect), and after the double of this time (to account for underestimation of development time or drift speed). The Barents Sea entrance was populated by particles after 42 days, but for most years investigated, few particles reached east of ~33°E, even within the doubled drift time (Fig. 4 and Fig. A4 in Appendix A). For the ten years with available survey data from the Kola transect, the relatively high abundances of *C. finmarchicus* copepodites observed were dominated by early copepodite stages (CI–CII) (Fig. 4). The estimated average development times for these stages were 25–30 days, thus less than the time needed to reach the Kola transect from the Norwegian Sea.

Compared to the other transects, the relatively longer and more variable egg–copepodite drift distance for the two Barents Sea entrance transects was driven by a higher and more variable drift speed, not development time (Fig. 5). These comparisons are based on straight-line distances from the back-calculated spawning locations to the survey stations, and are therefore generally underestimates of the true drift trajectory lengths and speeds. Due to a lower average temperature exposure during development, development time was on average longer for the two northernmost Norwegian Sea transects.

There were few consistent links between year-to-year variation in particle drift patterns and the NAO index (Table A1 in Appendix A). There was further a tendency that mean egg–CIV drift distance was higher for the Norwegian Sea transects in years with a positive NAO phase, but the correlation was only statistically significant ($p < 0.05$) for the NS·Open3 transect.

3.2. Sensitivity to the setup of the drift model

Releasing particles earlier or later (March 1st ± 15 days) increased or reduced the number of particles sampled at the Barents Sea transects, respectively (Table 1). The higher number of particles sampled with the earlier release date generally increased the number of spawning locations back-calculated in the vicinity of transects (Fig. A5 in Appendix A), decreasing the mean drift distance from egg to copepodite stage CIV. The number of particles reaching the Kola transect remained relatively low with the early release date (190, 116 of these being sampled in one single year, 1975).

Also releasing particles in areas with bottom depths from 300 to 500 m increased the total number of particles by 18%. Relative to this, the number of particles sampled at the Barents Sea transects increased substantially, in particular at the Kola transect (from 30 to 3002). For the two transects in the Barents Sea proper (North Cape and Kola), 99–100% of the back-calculated spawning locations were situated

Table 1
Percentage difference ($\pm$) between the results using the original model setup with release date 1st of March, drift depth 20 m, bottom depth of release area > 500 m and no horizontal diffusion (1), and the following alternatives: drift depth 10 m (2); drift depth 30 m (3); release date 15th of February (4); release date 15th of March (5); bottom depth of release area > 300 m (6); diffusion included in the drift model (7). The results are calculated using data for all years available, and include: total number of particles sampled per transect; mean drift distance from egg to CIV; mean development time from egg to CIV; percentage of back-calculated spawning locations situated on the shelf. Differences above 10% are shaded in grey. Values in brackets are absolute change.

| | | Percentage difference | | | | | | |
		1.Standard	2.Shallow	3.Deep	4.Early	5.Late	6.Shelf	7.Diffusion
Particles	NS.Open1	8324	1.4	1.5	0.9	2.9	41.2	1.1
	NS.Open2	11174	-3.5	-3.9	0.2	-0.8	27.5	-6.4
	NS.Open3	6683	13.3	-7.1	1.3	-2.8	15.6	-3.5
	BS.Enter1	3032	29.6	-14.0	35.0	-28.7	140.5	50.0
	BS.Enter2	6007	-2.8	3.8	10.7	-8.0	59.8	18.1
	N.Cape	3565	6.2	-1.5	63.8	-43.8	330.4	22.4
	Kola	30	-33.3	-20.0	533.3	-90.0	9906.7	-20.0
Distance	NS.Open1	191	0.5	-3.1	2.1	-3.1	-3.1	3.1
	NS.Open2	204	3.9	-4.9	-1.5	-6.4	1.0	1.5
	NS.Open3	201	14.4	-8.5	-0.5	-2.0	1.5	1.5
	BS.Enter1	257	3.1	4.7	-3.9	10.9	-0.4	3.1
	BS.Enter2	363	-5.0	0.3	-3.3	3.6	-3.6	-11.6
	N.Cape	200	-4.5	1.0	-13.5	10.5	-27.5	4.0
	Kola	294	3.1	2.7	-24.1	32.3	-50.0	7.5
Dev.time	NS.Open1	43	2.3	0.0	0.0	-7.0	0.0	2.3
	NS.Open2	53	0.0	0.0	0.0	-7.5	0.0	0.0
	NS.Open3	57	-1.8	0.0	1.8	-8.8	0.0	0.0
	BS.Enter1	41	-2.4	0.0	0.0	-2.4	0.0	2.4
	BS.Enter2	45	0.0	0.0	0.0	-2.2	0.0	2.2
	N.Cape	47	2.1	0.0	2.1	-2.1	8.5	2.1
	Kola	42	2.4	0.0	7.1	9.5	-7.1	28.6
% Shelf	NS.Open1	7	0.0	-14.3	14.3	-57.1	100.0	-42.9
	NS.Open2	0	0.0	0.0	0.0	0.0	(+1)	0.0
	NS.Open3	0	0.0	0.0	(+1)	0.0	(+1)	0.0
	BS.Enter1	67	6.0	0.0	6.0	-7.5	9.0	-20.9
	BS.Enter2	36	16.7	-2.8	2.8	-22.2	25.0	-11.1
	N.Cape	93	-1.1	1.1	3.2	-6.5	6.5	-1.1
	Kola	100	0.0	0.0	0.0	0.0	0.0	0.0

locally on the Barents Sea shelf, generally increasing the number of back-calculated spawning locations in the vicinity of the transects and decreasing the mean drift distance from egg to copepodite stage CIV (Table 1 and Fig. A6 in Appendix A). Including horizontal diffusion of particles increased the number of particles sampled, and the percentage of spawning locations situated off-shelf, for the Barents Sea entrance and North Cape transects, but not for the Kola transect. Changing the drift depth of particles did not systematically influence the results.

4. Discussion

The use of coupled physical-biological models to study plankton dynamics has gained much popularity the past decades (Miller, 2007). Here, we explicitly link and constrain hydrodynamic model results using observed biological data to map the origins of the new generation *C. finmarchicus* present in the Barents Sea in spring. The results indicate that spawning products are efficiently transported northward along the Norwegian shelf edge to the Barents Sea entrance. However, particles from the Norwegian Sea are unlikely to reach far into the Barents Sea proper (e.g. the Kola transect at 33°30′E) within the development time of observed copepodites. Based on these results, we suggest that *C. finmarchicus* stages CI–CIV present in the Barents Sea proper are unlikely to have been spawned in the Norwegian Sea, but may originate from local spawning components in the Barents Sea.

In the Norwegian Sea, the NAC follows the Norwegian continental shelf northward with high current speed (Blindheim, 2004). The three Norwegian Sea transects were situated near the shelf edge, with most back-calculated spawning locations predicted to be situated upstream along the "NAC highway". Continuing north, one branch of the NAC enters the Barents Sea. The main pathway is Bjørnøyrenna (Ingvaldsen and Loeng, 2009), a trench about halfway between the Norwegian coast and the island Bjørnøya. Many spawning locations for copepodites sampled at the Barents Sea entrance were located within Bjørnøyrenna
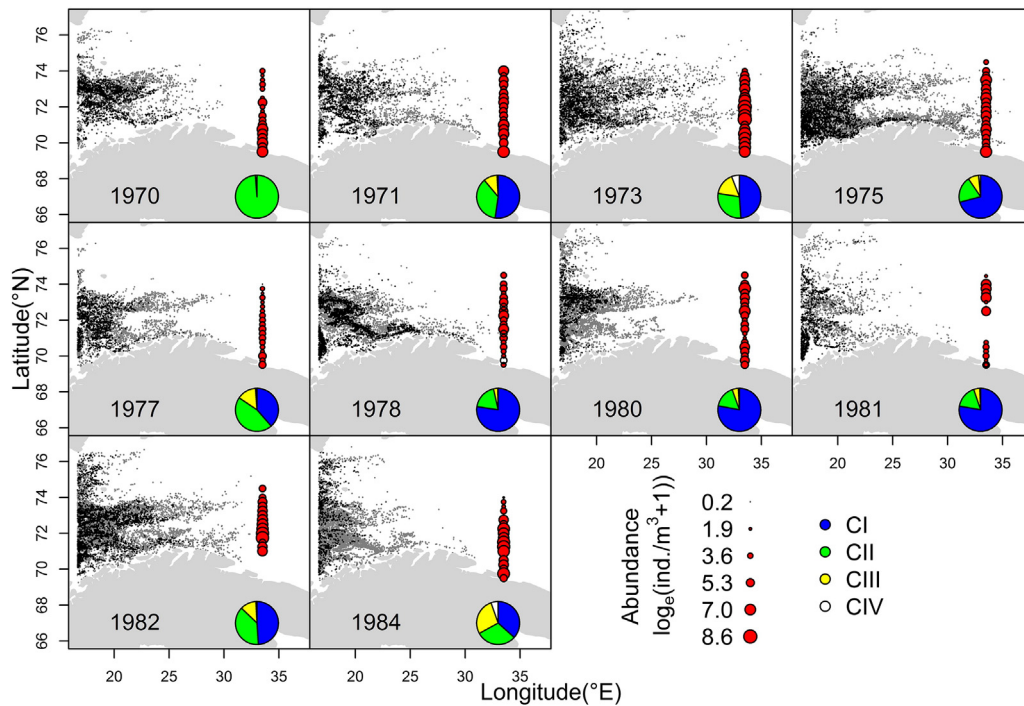
Fig. 4. Distribution of particles from the Norwegian Sea for 10 years of available Kola transect survey data. The panels show the distribution of particles initially released in the Norwegian Sea after 42 days of drift (black dots, i.e. the average estimated development time of stage CIV at the Kola transect), and the double of this time (grey dots). Survey stations at the Kola transect are shown as circles, with the size of the red circles indicating the observed pooled abundance of stages CI–CIV (natural logarithmic scale, zero observations indicated as empty circles). The pie charts show the distribution of the total observed abundance across developmental stages (CI: blue, CII: green, CIII: yellow, CIV: white). See Fig. A4 in Appendix A for particle distributions for all 31 years investigated. (For interpretation of the references to colour in this figure legend, the reader is referred to the web version of this article.)
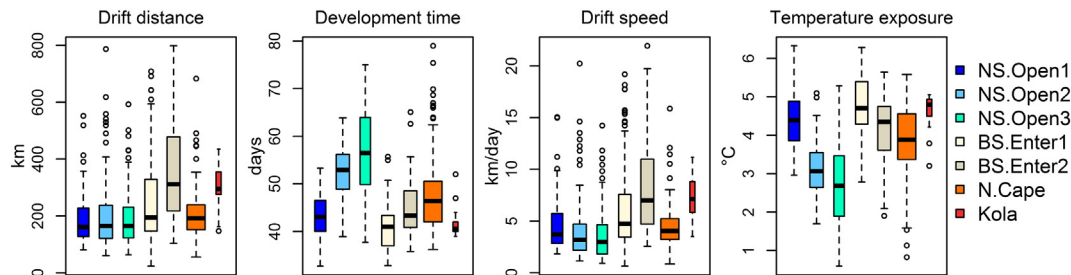
Fig. 5. Variation in estimated drift distance, development time, drift speed and temperature exposure from egg to copepodite stage CIV for the survey stations in the different transects, pooled for all years. The box plots show the following properties: the median (black horizontal line), the interquartile range (coloured box), the adjacent values (dashed whiskers) and outliers (open circles). The width of the boxes is proportional to the transect sample size (survey stations receiving particles with copepodite CIV observed). (For interpretation of the references to colour in this figure legend, the reader is referred to the web version of this article.)

or upstream along the Norwegian shelf edge, reflecting the importance of this pathway for transport from the Norwegian Sea to the Barents Sea. Opdal and Vikebø (2015) identified two other topographical features that appear to drive much of the *C. finmarchicus* transport from the Norwegian Sea to the Norwegian shelf, the Træna trough (67–70°N) and the Norwegian trench (62–64°N). Inspecting the total particle distribution per year, we found that in addition to Bjørnøyrenna, cross-shelf transport happened in various locations along the Norwegian continental shelf (results not shown). The recurrence of predicted spawning locations at ~67°N on the Norwegian continental shelf supports that the Træna trough acts as a cross-shelf route for *C. finmarchicus* which are in turn transported northwards to the Barents Sea entrance by the NCC.

Entering the Barents Sea, the NAC slows down (Ingvaldsen and Loeng, 2009), and few particles from the Norwegian Sea reached the Kola transect at 33°30′E. Nevertheless, *C. finmarchicus* copepodites were present at the time of the survey (Figs. 2 and 4). Several mechanisms might explain these findings: (1) presence of overwintering *C. finmarchicus* in the Barents Sea repopulating the area in spring; (2) prolonged transport of adult specimens prior to spawning; (3) advection of adult specimens from overwintering sites in fjords along the Norwegian coast; or (4) model underestimation of transport into the Barents Sea.

It is debated to which extent the Barents Sea is used for overwintering by *C. finmarchicus* (e.g. Arashkevich et al., 2002; Tande, 1991), or if the new generation appearing in spring and summer is dependent on advection from the Norwegian Sea (e.g. Edvardsen et al., 2003b; Skjoldal and Rey, 1989; Slagstad and Tande, 2007). It has been argued that due to the risks of being transported north outside favourable environmental conditions (Aksnes and Blindheim, 1996; Melle and Skjoldal, 1998), or being eaten by visual predators in the shallow shelf areas during winter (Bagøien et al., 2001; Torgersen and Huse, 2005), *C. finmarchicus* is an expatriate in the Barents Sea. Further, the variability in zooplankton biomass in the Barents Sea has been shown to correlate with the strength of Atlantic water inflow (Helle and Pennington, 1999), and advected zooplankton biomass from the Norwegian Sea has been estimated to outnumber local production four times (Edvardsen et al., 2003b).

On the other hand, recent estimates indicate that local production is the most important contributor to *C. finmarchicus* production in the Barents Sea proper (Dalpadado et al., 2012; Skaret et al., 2014). Observations of overwintering *C. finmarchicus* in the Barents Sea (Dvoretsky and Dvoretsky, 2015; Manteifel, 1941; Pedersen, 1995) and a positive correlation between the inflow of Atlantic water one year and *C. finmarchicus* biomass in the Barents Sea the following year (Dvoretsky and Dvoretsky, 2014) support that *C. finmarchicus* overwinters in the Barents Sea. The species also displays a broad range of overwintering depths in the Northwest Atlantic (Head and Pepin, 2007), including shelf areas (100–300 m) and shallow waters in the Greenland Sea where cold Arctic Intermediate Water reaches the surface (Dale et al., 1999). Population genetic analyses have indicated that *C. finmarchicus* in the Barents Sea belongs to a distinct population, genetically differentiated from the Norwegian Sea population (Unal and Bucklin, 2010). The mechanisms behind the differentiation are unknown, but local overwintering and spawning of *C. finmarchicus* in the Barents Sea could potentially sustain this population structuring.

Seeding particles earlier, thereby extending the time available to drift into the Barents Sea, increased the number of particles reaching the Barents Sea transects. Still, copepodites observed at the Barents Sea transects were predicted to have been spawned on the Barents Sea shelf (i.e. 96–100% of the back-calculated spawning locations for the North Cape and Kola transects). Depending on the longevity of *C. finmarchicus* females, the new generation present in the Barents Sea could originate from females advected onto the shelf after emerging from overwintering in the Norwegian Sea. The mortality rate of *C. finmarchicus* females in the Northeast Atlantic has been estimated to range from 0.02 d^{-1} (Melle et al., 2014), implying an average life span of ~50 days after reaching the adult stage, to 0.14 d^{-1} (Dvoretsky and Dvoretsky, 2013), implying an average life span of only 9 days. In a low mortality regime, females from the Norwegian Sea may thus drift onto the western Barents Sea shelf (Fig. 4) and spawn eggs that can continue to drift north and eastward. However, even when particles were released in mid-February, 2–4 weeks earlier than the estimated arrival of *C. finmarchicus* females in upper waters in the Northeast Atlantic (Heath, 1999; Melle et al., 2014), 77% of the Kola stations received no particles within the time of the survey.

C. finmarchicus also overwinters in fjords along the Norwegian coast (Espinasse et al., 2016; Kaartvedt, 1996), and eggs spawned by females ascending from fjords could potentially be advected with the NCC into the southern Barents Sea. Previous modelling studies have shown that both *C. finmarchicus* from the Norwegian continental shelf (Torgersen and Huse, 2005) and cod eggs and larvae from coastal spawning grounds as far south as 58°N (Opdal et al., 2011) end up in the Barents Sea with the NCC. As inshore and fjord areas are not well resolved in the hydrodynamic model used here, it was not feasible to include fjords in the initial seeding distribution, but it should be considered in future work.

Finally, while our results suggest that the Norwegian Sea is not the only source of *C. finmarchicus* copepodites observed in the Barents Sea, the ocean model might underestimate transport from the Norwegian Sea to the Barents Sea. Advancing the grid resolution from 20 km to 4.5 km increased cross-shelf transport (Samuelsen et al., 2009; Torgersen and Huse, 2005), but is unknown whether the current resolution is sufficient for realistically reproducing cross-shelf transport. Including horizontal diffusion in the drift model appeared to increase cross-shelf transport (Table 1), but not the eastward drift of particles within the Barents Sea. According to Lien et al. (2013), the ocean model tends to underestimate current strength in some areas, and be more strongly controlled by topography, which in turn could affect the model's ability to move particles across topographical structures such as the Norwegian continental shelf break. At the same time, the NAC speed is rather overestimated close to the shelf break (Melsom and Gusdal, 2015), but no systematic under- or overestimation of

current speed has been detected in the Barents Sea (A. Melsom, personal communication).

Current velocities in the Barents Sea opening typically range from 0 to 20 cm s^{-1} (Lien et al., 2013). At the higher range of these observations, the distance from the Barents Sea shelf edge to the Kola transect (~600 km at the minimum) could in theory be covered within the development time of copepodite stages CIII and CIV. The straight-line drift speeds displayed in Fig. 5 are mainly in the lower range of these values, however, particles are typically caught by eddies and follow irregular trajectories. As an example, see the available supplementary animation showing the particle drift trajectories from the release day to sampling at the Kola transect in 1975 (online version only). The immediate drift speeds displayed in this example are within the range of previous observations (on average 13 cm s^{-1}). I.e. besides drift speed, the complexity of the drift trajectories slow down eastward transport in the Barents Sea.

The estimated spawning locations varied inter-annually (Fig. A2), likely driven by variation in ocean circulation patterns. The NAC tends to be stronger during NAO-positive years (Blindheim, 2004; Sandø et al., 2010), thereby increasing Atlantic water inflow and temperatures in the Barents Sea (Stenseth et al., 2002). Indeed, copepodite development times in this study, estimated from temperatures along the particles' trajectories, generally decreased during NAO-positive years. But while average egg–copepodite drift distance as expected tended to be higher for the Norwegian Sea transects during NAO-positive years, this relationship did not emerge for the Barents Sea transects. Although a positive NAO is associated with a stronger NAC, Atlantic water influx in the Barents Sea is ultimately largely determined by wind fields in the Barents Sea opening, and the effect of local atmospheric conditions can in periods reduce the link between the NAO and Barents Sea climate (Ingvaldsen and Loeng, 2009).

We used a forward-in-time trajectory approach (FITT), seeding a large number of uniformly distributed particles in the Norwegian Sea. Seeding particles at the stations and drifting backwards in time (BITT) would be more computationally efficient, and circumvent some uncertainties, such as the release date and the low number of particles reaching the Kola transect. If diffusion is excluded (as in our main simulation), a single particle BITT should equal a FITT (Batchelder, 2006), but to get a measure of variation in potential origins, diffusion should not be ignored in BITT (Batchelder, 2006; Christensen et al., 2007). Including diffusion leads to increased uncertainty as time progresses backwards, and BITT results should be interpreted as spatial probability fields, likely being less conservative than FITT results (Christensen et al., 2007; Pepin et al., 2013). While we here test whether C. finmarchicus in the Barents Sea might originate from spawning areas in the Norwegian Sea, a known core distribution area of the species, BITT results are driven solely by modelled current fields and may point to less realistic origins (Pepin et al., 2013). Nevertheless, comparing results from both approaches may expand our knowledge of the origins of C. finmarchicus in the Barents Sea.

In an earlier modelling study, particles representing C. finmarchicus sampled in the western Barents Sea in July were found to originate chiefly from a narrow band off the shelf break (Slagstad and Tande, 2007). Our results support that this area is an important source for C. finmarchicus in the Barents Sea entrance. However, while the former study tracked the origin of the G0 generation, the present study shows, by coupling drift modelling with biological data, that on-shelf transport is unlikely to populate more eastern parts of the Barents Sea within the development time of G1 copepodites, or, depending on the mortality rate, within the life time of adult females. Releasing particles in shallower areas, including parts of the Barents Sea, increased the number of particles reaching the Barents Sea transects by several orders of magnitude, supporting that C. finmarchicus copepodites present here in spring are spawned on the Barents Sea shelf, not in the Norwegian Sea. While modelling studies have suggested that due to local transport dynamics, C. finmarchicus in the Barents Sea would likely go extinct if advection from the Norwegian Sea completely stopped (Skaret et al., 2014), our results support that C. finmarchicus dynamics in the Barents Sea is not, at least in the short-term, solely driven by advection from the Norwegian Sea, but by local spawning.

Supplementary data to this article can be found online at http://dx.doi.org/10.1016/j.jmarsys.2016.09.010.

Acknowledgements

References

Ådlandsvik, B., Sundby, S., 1994. Modelling the transport of cod larvae from the Lofoten area. ICES Mar. Sci. Symp. 198, 379–392.

Aksnes, D.L., Blindheim, J., 1996. Circulation patterns in the North Atlantic and possible impact on population dynamics of Calanus finmarchicus. Ophelia 44, 7–28. http://dx.doi.org/10.1080/00785326.1995.10429836.

Arashkevich, E., Wassmann, P., Pasternak, A., Wexels Riser, C., 2002. Seasonal and spatial changes in biomass, structure, and development progress of the zooplankton community in the Barents Sea. J. Mar. Syst. 38, 125–145. http://dx.doi.org/10.1016/S0924-7963(02)00173-2.

Bagøien, E., Kaartvedt, S., Aksnes, D.L., Eiane, K., 2001. Vertical distribution and mortality of overwintering Calanus. Limnol. Oceanogr. 46, 1494–1510. http://dx.doi.org/10.4319/lo.2001.46.6.1494.

Batchelder, H.P., 2006. Forward-in-time−/backward-in-time-trajectory (FITT/BITT) modeling of particles and organisms in the coastal ocean*. J. Atmos. Ocean. Technol. 23, 727–741. http://dx.doi.org/10.1175/JTECH1874.1.

Blindheim, J., 2004. Oceanography and climate. In: Skjoldal, H.R. (Ed.), The Norwegian Sea Ecosystem. Tapir Academic Press, Trondheim, pp. 65–96.

Bryant, A.D., Hainbucher, D., Heath, M., 1998. Basin-scale advection and population persistence of Calanus finmarchicus. Fish. Oceanogr. 7, 235–244. http://dx.doi.org/10.1046/j.1365-2419.1998.00074.x.

Campbell, R.G., Wagner, M.M., Teegarden, G.J., Boudreau, C.A., Durbin, E.G., 2001. Growth and development rates of the copepod Calanus finmarchicus reared in the laboratory. Mar. Ecol. Prog. Ser. 221, 161–183. http://dx.doi.org/10.3354/meps221161.

Christensen, A., Daewel, U., Jensen, H., Mosegaard, H., St John, M., Schrum, C., 2007. Hydrodynamic backtracking of fish larvae by individual-based modelling. Mar. Ecol. Prog. Ser. 347, 221–232. http://dx.doi.org/10.3354/meps06980.

Dale, T., Kaartvedt, S., 2000. Diel patterns in stage-specific vertical migration of Calanus finmarchicus in habitats with midnight sun. ICES J. Mar. Sci. 57, 1800–1818. http://dx.doi.org/10.1006/jmsc.2000.0961.

Dale, T., Bagøien, E., Melle, W., Kaartvedt, S., 1999. Can predator avoidance explain varying overwintering depth of Calanus in different oceanic water masses? Mar. Ecol. Prog. Ser. 179, 113–121. http://dx.doi.org/10.3354/meps179113.

Dalpadado, P., Ingvaldsen, R.B., Stige, L.C., Bogstad, B., Knutsen, T., Ottersen, G., Ellertsen, B., 2012. Climate effects on Barents sea ecosystem dynamics. ICES J. Mar. Sci. 69, 1303–1316. http://dx.doi.org/10.1093/icesjms/fss063.

Dvoretsky, V.G., Dvoretsky, A.G., 2013. The mortality levels of two common copepods in the Barents Sea. Vestn. MGTU 16, 460–465 (in Russian). UDC 595.344.1 268.45).

Dvoretsky, V.G., Dvoretsky, A.G., 2014. Interannual fluctuations of zooplankton in the Kola section (Barents Sea) in relation to environmental factors. Biol. Bull. 41, 378–386. http://dx.doi.org/10.1134/S1062359014040049.

Dvoretsky, V.G., Dvoretsky, A.G., 2015. Early winter mesozooplankton of the coastal south-eastern Barents Sea. Estuar. Coast. Shelf Sci. 152, 116–123. http://dx.doi.org/10.1016/j.ecss.2014.11.016.

Edvardsen, A., Slagstad, D., Tande, K.S., Jaccard, P., 2003a. Assessing zooplankton advection in the Barents Sea using underway measurements and modelling. Fish. Oceanogr. 12, 61–74. http://dx.doi.org/10.1046/j.1365-2419.2003.00219.x.

Edvardsen, A., Tande, K.S., Slagstad, D., 2003b. The importance of advection on production of Calanus finmarchicus in the Atlantic part of the Barents Sea. Sarsia 88, 261–273. http://dx.doi.org/10.1080/003648203103342867.

Espinasse, B., Basedow, S., Tverberg, V., Hattermann, T., Eiane, K., 2016. A major Calanus finmarchicus overwintering population inside a deep fjord in northern Norway: implications for cod larvae recruitment success. J. Plankton Res. 0, 1–6. http://dx.doi.org/10.1093/plankt/fbw024.

Gjøsæter, H., 2009. Commercial fisheries (fish, seafood and marine mammals). In: Sakshaug, E., Johnsen, G., Kovacs, K. (Eds.), Ecosystem Barents Sea. Tapir Academic Press, Trondheim, Norway, pp. 373–414.

Haidvogel, D.B., Arango, H., Budgell, W.P., Cornuelle, B.D., Curchitser, E., Di Lorenzo, E., Fennel, K., Geyer, W.R., Hermann, A.J., Lanerolle, L., Levin, J., McWilliams, J.C., Miller, A.J., Moore, A.M., Powell, T.M., Shchepetkin, A.F., Sherwood, C.R., Signell, R.P., Warner, J.C., Wilkin, J., 2008. Ocean forecasting in terrain-following coordinates: formulation and skill assessment of the Regional Ocean Modeling System. J. Comput. Phys. 227, 3595–3624. http://dx.doi.org/10.1016/j.jcp.2007.06.016.

Head, E., Pepin, P., 2007. Variations in overwintering depth distributions of Calanus finmarchicus in the slope waters of the NW Atlantic continental shelf and the Labrador Sea. J. Northwest Atl. Fish. Sci. 39, 49–69. http://dx.doi.org/10.2960/J.v39.m600.

Heath, M.R., 1999. The ascent migration of Calanus finmarchicus from overwintering depths in the Faroe-Shetland Channel. Fish. Oceanogr. 8, 84–99. http://dx.doi.org/10.1046/j.1365-2419.1999.00013.x.

Helle, K., 2000. Distribution of the copepodite stages of Calanus finmarchicus from Lofoten to the Barents Sea in July 1989. ICES J. Mar. Sci. 57, 1636–1644. http://dx.doi.org/10.1006/jmsc.2000.0954.

Helle, K., Pennington, M., 1999. The relation of the spatial distribution of early juvenile cod (Gadus morhua L.) in the Barents Sea to zooplankton density and water flux during the period 1978–1984. ICES J. Mar. Sci. 56, 15–27. http://dx.doi.org/10.1006/jmsc.1998.0427.

Hernroth, L., 1987. Sampling and filtration efficiency of two commonly used plankton nets. A comparative study of the Nansen net and the Unesco WP 2 net. J. Plankton Res. 9, 719–728. http://dx.doi.org/10.1093/plankt/9.4.719.

Hjøllo, S.S., Huse, G., Skogen, M.D., Melle, W., 2012. Modelling secondary production in the Norwegian Sea with a fully coupled physical/primary production/individual-based Calanus finmarchicus model system. Mar. Biol. Res. 8, 508–526. http://dx.doi.org/10.1080/17451000.2011.642805.

Hurrell, J., National Center for Atmospheric Research Staff, 2013. The Climate Data Guide: Hurrell North Atlantic Oscillation (NAO) Index (PC-Based)" [WWW Document]. URL https://climatedataguide.ucar.edu/climate-data/hurrell-north-atlantic-oscillation-nao-index-pc-based.

Ingvaldsen, R.B., Loeng, H., 2009. Physical oceanography. In: Sakshaug, E., Johnsen, G., Kovacs, K. (Eds.), Ecosystem Barents Sea. Tapir Academic Press, Trondheim, pp. 33–64.

Kaartvedt, S., 1996. Habitat preference during overwintering and timing of seasonal vertical migration of Calanus finmarchicus. Ophelia 44, 145–156. http://dx.doi.org/10.1080/00785326.1995.10429844.

Kvile, K.Ø., Dalpadado, P., Orlova, E., Stenseth, N.C., Stige, L.C., 2014. Temperature effects on Calanus finmarchicus vary in space, time and between developmental stages. Mar. Ecol. Prog. Ser. 517, 85–104. http://dx.doi.org/10.3354/meps11024.

Lien, V.S., Gusdal, Y., Albretsen, J., Melsom, A., Vikebø, F., 2013. Evaluation of a Nordic Seas 4 km numerical ocean model hindcast archive (SVIM), 1960–2011. Fisk. og Havet 7, 1–80.

Loeng, H., 1991. Features of the physical oceanographic conditions of the Barents Sea. Polar Res. 10, 5–18. http://dx.doi.org/10.1111/j.1751-8369.1991.tb00630.x.

Loeng, H., Drinkwater, K., 2007. An overview of the ecosystems of the Barents and Norwegian Seas and their response to climate variability. Deep Sea Res. Part II Top. Stud. Oceanogr. 54, 2478–2500. http://dx.doi.org/10.1016/j.dsr2.2007.08.013.

Manteifel, B.P., 1941. Plankton and herring in the Barents Sea. Tr. PINRO. Trans. Knipovich Polar Sci. Inst. Sea-Fisheries Oceanogr. Murm. 7, 125–218 in Russian.

Melle, W., Skjoldal, H., 1998. Reproduction and development of Calanus finmarchicus. C. glacialis and C. hyperboreus in the Barents Sea. Mar. Ecol. Prog. Ser. 169, 211–228. http://dx.doi.org/10.3354/meps169211.

Melle, W., Ellertsen, B., Skjoldal, H.R., 2004. Zooplankton: the link to higher trophic levels. In: Skjoldal, H.R. (Ed.), The Norwegian Sea Ecosystem. Tapir Academic Press, Trondheim, pp. 137–202.

Melle, W., Runge, J., Head, E., Plourde, S., Castellani, C., Licandro, P., Pierson, J., Jonasdottir, S., Johnson, C., Broms, C., Debes, H., Falkenhaug, T., Gaard, E., Gislason, A., Heath, M., Niehoff, B., Nielsen, T.G., Pepin, P., Stenevik, E.K., Chust, G., 2014. The North Atlantic Ocean as habitat for Calanus finmarchicus: environmental factors and life history traits. Prog. Oceanogr. 129, 244–284. http://dx.doi.org/10.1016/j.pocean.2014.04.026.

Melsom, A., Gusdal, Y., 2015. Evaluation of Ocean Currents From Model Simulations (METreport No. 14/2015). Norwegian Meterological Institute.

Miller, T., 2007. Contribution of individual-based coupled physical–biological models to understanding recruitment in marine fish populations. Mar. Ecol. Prog. Ser. 347, 127–138. http://dx.doi.org/10.3354/meps06973.

Nesterova, V.N., 1990. Plankton Biomass Along the Drift Route of Cod Larvae (Reference Material). PINRO, Murmansk in Russian.

Nichols, J.H., Thompson, A.B., 1991. Mesh selection of copepodite and nauplius stages of four calanoid copepod species. J. Plankton Res. 13, 661–671. http://dx.doi.org/10.1093/plankt/13.3.661.

Niehoff, B., Klenke, U., Hirche, H., Irigoien, X., Head, R., Harris, R., 1999. A high frequency time series at Weathership M, Norwegian Sea, during the 1997 spring bloom: the reproductive biology of Calanus finmarchicus. Mar. Ecol. Prog. Ser. 176, 81–92. http://dx.doi.org/10.3354/meps176081.

Opdal, A.F., Vikebø, F.B., 2015. Long-term stability in modelled zooplankton influx could uphold major fish spawning grounds on the Norwegian continental shelf. Can. J. Fish. Aquat. Sci. 1–8. http://dx.doi.org/10.1139/cjfas-2014-0524.

Opdal, A.F., Vikebø, F., Fiksen, Ø., 2011. Parental migration, climate and thermal exposure of larvae: spawning in southern regions gives Northeast Arctic cod a warm start. Mar. Ecol. Prog. Ser. 439, 255–262. http://dx.doi.org/10.3354/meps09335.

Orlova, E.L., Boitsov, V.D., Nesterova, V.N., 2010. The Influence of Hydrographic Conditions on the Structure and Functioning of the Trophic Complex Plankton – Pelagic Fishes – Cod, Knipovich's Polar Research Institute of Marine Fisheries and Oceanography (PINRO), Murmansk. Knipovich's Polar Research Institute of Marine Fisheries and Oceanography (PINRO), Murmansk.

Ottersen, G., Stenseth, N.C., 2001. Atlantic climate governs oceanographic and ecological variability in the Barents Sea. Limnol. Oceanogr. 46, 1774–1780. http://dx.doi.org/10.4319/lo.2001.46.7.1774.

Pedersen, G., 1995. Why does a component of Calanus finmarchicus stay in the surface waters during the overwintering period in high latitudes? ICES J. Mar. Sci. 52, 523–531. http://dx.doi.org/10.1016/1054-3139(95)80066-2.

Pepin, P., Han, G., Head, E.J., 2013. Modelling the dispersal of Calanus finmarchicus on the Newfoundland shelf: implications for the analysis of population dynamics from a high frequency monitoring site. Fish. Oceanogr. 22, 371–387. http://dx.doi.org/10.1111/fog.12028.

Pyper, B.J., Peterman, R.M., 1998. Comparison of methods to account for autocorrelation in correlation analyses of fish data. Can. J. Fish. Aquat. Sci. 55, 2127–2140. http://dx.doi.org/10.1139/cjfas-55-9-2127.

Quenouille, M.H., 1952. Associated Measurements. Butterworth, London.

Reistad, M., Breivik, Ø., Haakenstad, H., Aarnes, O.J., Furevik, B.R., Bidlot, J.-R., 2011. A high-resolution hindcast of wind and waves for the North Sea, the Norwegian Sea, and the Barents Sea. J. Geophys. Res. 116, C05019. http://dx.doi.org/10.1029/2010JC006402.

Rey, F., 2004. Phytoplankton: the grass of the sea. In: Skjoldal, H.R. (Ed.), The Norwegian Sea Ecosystem. Tapir Academic Press, Trondheim, pp. 97–136.

Samuelsen, A., Huse, G., Hansen, C., 2009. Shelf recruitment of Calanus finmarchicus off the west coast of Norway: role of physical processes and timing of diapause termination. Mar. Ecol. Prog. Ser. 386, 163–180. http://dx.doi.org/10.3354/meps08060.

Sandø, A.B., Nilsen, J.E.Ø., Gao, Y., Lohmann, K., 2010. Importance of heat transport and local air-sea heat fluxes for Barents Sea climate variability. J. Geophys. Res. 115, C07013. http://dx.doi.org/10.1029/2009JC005884.

Skaret, G., Dalpadado, P., Hjøllo, S.S., Skogen, M.D., Strand, E., 2014. Calanus finmarchicus abundance, production and population dynamics in the Barents Sea in a future climate. Prog. Oceanogr. 125, 26–39. http://dx.doi.org/10.1016/j.pocean.2014.04.008.

Skjoldal, H.R., Rey, F., 1989. Pelagic production and variability of the Barents Sea ecosystem. In: Sherman, K., Alexander, L.M. (Eds.), Biomass Yields and Geography of Large Marine Ecosystems. American Association for the Advancement of Science. Selected Symposia, pp. 241–286.

Slagstad, D., Tande, K.S., 2007. Structure and resilience of overwintering habitats of Calanus finmarchicus in the Eastern Norwegian Sea. Deep Sea Res. Part II Top. Stud. Oceanogr. 54, 2702–2715. http://dx.doi.org/10.1016/j.dsr2.2007.08.024.

Stenevik, E.K., Melle, W., Gaard, E., Gislason, A., Broms, C.T.Å., Prokopchuk, I., Ellertsen, B., 2007. Egg production of Calanus finmarchicus — a basin-scale study. Deep Sea Res. Part II Top. Stud. Oceanogr. 54, 2672–2685. http://dx.doi.org/10.1016/j.dsr2.2007.08.027.

Stenevik, E.K., Vølstad, J.H., Høines, Å., Aanes, S., Óskarsson, G.J., Jacobsen, J.A., Tangen, Ø., 2015. Precision in estimates of density and biomass of Norwegian spring-spawning herring based on acoustic surveys. Mar. Biol. Res. 11, 449–461. http://dx.doi.org/10.1080/17451000.2014.995672.

Stenseth, N.C., Mysterud, A., Ottersen, G., Hurrell, J.W., Chan, K.-S., Lima, M., 2002. Ecological effects of climate fluctuations. Science 297, 1292–1296. http://dx.doi.org/10.1126/science.1071281.

Tande, K.S., 1991. Calanus in North Norwegian fjords and in the Barents Sea. Polar Res. 10, 389–408. http://dx.doi.org/10.1111/j.1751-8369.1991.tb00661.x.

Torgersen, T., Huse, G., 2005. Variability in retention of Calanus finmarchicus in the Nordic Seas. ICES J. Mar. Sci. 62, 1301–1309. http://dx.doi.org/10.1016/j.icesjms.2005.05.016.

Unal, E., Bucklin, A., 2010. Basin-scale population genetic structure of the planktonic copepod Calanus finmarchicus in the North Atlantic Ocean. Prog. Oceanogr. 87, 175–185. http://dx.doi.org/10.1016/j.pocean.2010.09.017.

Unstad, K.H., Tande, K.S., 1991. Depth distribution of Calanus finmarchicus and C. glacialis in relation to environmental conditions in the Barents Sea. Polar Res. 10, 409–420. http://dx.doi.org/10.1111/j.1751-8369.1991.tb00662.x.